XRF and μ-tomography investigations of gold jewellery from the Middle Bronze Age from the Nerkin Naver burial mound (Armenia)

Hakob Simonyan[1], V. Kocharyan[2], V. Margaryan[2], E. Minasyan[3], Yuri Cherepennikov [2,4]

[1] Scientific Research Center of Historical &
Cultural Heritage of Ministry of Education, Science, Culture and Sport of RA, 1/3 Buzand Str., Yerevan 0010 - haksimon@gmail.com
[2] Institute of Applied Problems of Physics NAS RA Hr.Nersessian Street 25, Yerevan, 0014, Republic of Armenia
[3] Yerevan State University (YSU) Armenia, 0025, Yerevan, Alek Manukyan St., 1 Building
[4] National Research Tomsk Polytechnic University, Lenina Avenue 30, Tomsk, 634050, Russia

Keywords: Burial Mound, Gold Jewellery, X-Ray Fluorescence, μ-Tomography.

Abstract

The article summarizes complex studies on X-Ray Fluorescence (XRF), μ-tomography, and elemental analysis of a unique golden artefact from burial mound No. 10 of Nerkin Naver (Armenia), which according to the results of radiocarbon analysis is a contemporary of the epoch when the masterpieces of jewellery art of the III dynasty of Ur of the Sumero-Akkadian kingdom of Southern Mesopotamia (2111-2003 BC) were created. A jewelry obtained in tis burial mound and dated back to 2133-1954 BC were investigated to clarify the design, composition and manufacturing technique. We performed comprehensively analysis of the artifact using modern methods of the natural sciences. The results showed that this jewelry is made of gold with more than 80% of purity and infilled by the gypsum. Tomographic studies allowed suggested particular way of production and visualize the structure of golden shell and infill material separately. Basing on the suggestions about artefact composition and structures, its mass was calculated. Calculated and physically measured mass are in good accordance.

1. Introduction

One of the most significant challenges in the archaeology of Armenia and the South Caucasus is the study of the monuments of the "Early Kurgan" culture (2300-2000 BCE), spanning from the end of the Kura-Araxes culture Early Bronze Age. There is a widespread stereotype that archaeological monuments on the territory of Republic of Armenia date back to Trialeti stage – the second period of the "Early Kurgan" culture (Avetisyan, 2020). This point of view requires reassessment, given the significant number of newly discovered monuments dating back to the last quarter of the 3rd millennium B.C. This stratum of monuments with the richest artifacts provides a solid basis for revising the chronological framework of archaeological cultures and historical events of ancient Armenia. A comprehensive analysis of the archaeological sources provides ample evidence for the existence of an early Kurgan culture and the emergence of the institution of royal authority in the third quarter of the 3rd millennium B.C. in the Armenian Highland.

In order to solve the above-mentioned problem, it is necessary to conduct further studies of the extensive cemetery in Nerqin Naver Amongst the excavated monuments, one the most significant is the grave N10, which is a unique in terms of discovered burial rites, original and luxurious gifts, as well as the variety of animals sacrificed, including a horse. As a result of comprehensive research, this tomb could become a valuable source of historical reconstructions, shedding light on new previously overlooked aspects of our past. This article deals with a unique masterpiece of jewelry art, which is preserved almost entirely and required non-invasive study of its structural composition and manufacturing technique. The study of red deposition on the surface of the gold ornament was also important. The article deals with the analysis of this ancient goldsmithing masterpiece using methods of XRF and μ-tomography.

Application of modern experimental techniques for studying of cultural heritage, without damaging artefacts, gets more and more interests from researchers around the world. X-ray based techniques a particularly promising for this purpose. A number of studies are performed via X-Ray Fluorescence (XRF) and tomography analysis (Ceccarelli et al., 2022, Dabagov and Gladkikh, 2019, Morigi et al., 2010, Gonzalez et al., 2020, Ruvalcaba Sil et al., 2010, Vaggelli and Cossio, 2012, Brunello et al., 2021). However, huge number of different samples still need to be investigated to enrich knowledge in different scientific fields, e.g. archeology.

Figure 1. Location of the necropolis of Nerkin Naver.

In this study we summarize complex studies on XRF, μ-

This contribution has been peer-reviewed.
https://doi.org/10.5194/isprs-archives-XLVIII-2-W5-2024-123-2024 | © Author(s) 2024. CC BY 4.0 License.

Figure 2. Discovered burial mounds at the necropolis of Nerkin Naver.

tomography, and elemental analysis of a unique golden artefact from burial mound No. 10 of Nerkin Naver (Armeniam, Figure 1) performed at Institute of Applied Problems of Physics (Yerevan, Armenia). The artefact is synchronous to masterpieces of gold-making of the III dynasty of Ur of the Sumerian-Akkadian kingdom of Southern Mesopotamia (2111-2003 BC) according to the result of radiocarbon analysis. This Age corresponds to grandiose historical and cultural shifts at ancient East followed by creation of highly developed states with royal workshops in which professional craftsmen created their exquisite masterpieces. According to archaeological research, ancient Armenia was included in these global processes. One of the core monuments of the Middle Bronze Age of Armenia is the necropolis of Nerkin Naver, which is located 30 km northwest of the capital of the Republic of Armenia - Yerevan, less than 5 km west of the city of Ashtarak - the centre of the Aragatsotn region, at the junction of the lands of the villages of Parpi, Oshakan and Voskevaz, on the plateau of the left bank of the Shakhverd River, at an altitude of 1050–1100 m above sea level (Fig. 1).

Since 2002, the archaeological expedition of the "Research Center for Historical and Cultural Heritage" of the Ministry of Education, Science, Culture and Sports of the Republic of Armenia under the leadership of H.Ye. Simonyan began excavations and a comprehensive study of the monument (Simonyan, 2019). Currently, 18 burial mounds have been discovered, which contained individual burials of the aristocracy of that time (Fig.2).

A number of artefacts was found: weapons (rapier, spear, daggers, arrowheads, shtandart, stone tools, hewn basalt bowls); beads and amulets of different models and colours made of gold, silver, bronze, agate, jet gemstone - black amber, carnelian, rock crystal, agalmatolite; gold and glass wheel models; gold plates covering furniture and wooden objects; seashells exported from the Persian Gulf and others. Spherical beads with cone-shaped and hemispherical spikes are commonly faced. A large arsenal of technological approaches was used in the manufacture of gold samples: cold and hot forging, wax casting, soldering (welding), grinding, chasing, stamping, engraving, polishing, etc. Colouring gold specimens red was also common. To clarify the design, composition and manufacturing technique of one of these jewelleries, dating back to 2133-1954 BC (CEZA, Lab Nr MAMS 52762, bone) we performed comprehensively analysis of the artefact using modern methods of the natural sciences.

2. XRF Studies

Experimental studies were carried out to determine the composition and internal structure of the archaeological sample. The sample is close to spherical in shape, the shell is made of yellow metal, damaged in several areas, in the damaged areas the sample is filled with a grey substance with a granular structure, presumably gypsum, there are multiple protrusions ("spikes") on the shell, at the top and bottom of the sample there are "fastenings", made of metal (Figure 2). Partially there are traces of red paint on the shell, probably cinnabar. The section radius in the central part is approximately 35 mm, height is 38 mm.

To determine the materials that make up the sample, XRF ana-

Figure 3. Burial mound Nerkin Naver, tomb N10.

Figure 4. Appearance of the archaeological specimen.

lysis with an X-ray tube and X-ray spectrometer based on silicon drift detector (AMPTEK-SDD) was performed. The detector allows registration of gamma-quanta up to 40 keV. XRS-FP2 software was used to acquire and analyze fluorescence spectrum. Probe beam was generated by X-ray source based on Mo X-ray tube with operating parameters of 30 kV and 10 mA. Fluorescence spectra were measured for two cases: X-ray beam was directed at the metal shell and at the internal part in area of damaged shell.

Figure 5 demonstrates spectral measurement of fluorescence from metal shell area. The most intensive characteristic X-ray lines detected in experiment were $L\alpha$, $L\beta$, $L\gamma$ of Au; $K\alpha$ and $K\beta$ of Ag and Cu. Mo lines in spectrum are generated in anode of X-ray tube, while Fe lines in slit collimators. Therefore, it was concluded that metal shell is made of mainly gold with small amounts of copper and silver.

Next step was to measure fluorescence spectrum from a specimen part in area of damaged shell. It was our suggestion that the specimen was filled with gypsum. Gypsum is a mixture of $CaSO_4$, which can exist in various modifications with water of crystallization. The energies of $K\alpha$ characteristic X-ray for Ca, S, and O are 3.7, 2.3, and 0.5 keV respectively, that are very low values and, consequently, acquiring them in presence of air between measured sample and a detector is a quite hard task. Figure 6 demonstrates measured spectrum; it can be seen that this spectrum contains Ca K-line. However, the intensity of this line is very low that is caused by X-ray attenuation in air. Moreover, in this spectrum we saw intensive Au lines that

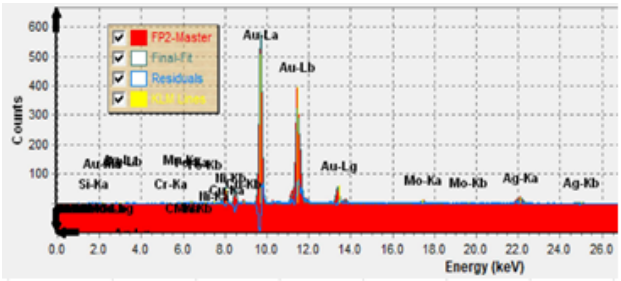

Component Table						
Component	Type	Conc.	Error	Units	Mole%	Error
Cr	Calc	0.115	0.135	wt.%	0.336	0.396
Mn	Calc	0.404	0.264	wt.%	1.12	0.732
Fe	Calc	1.364	0.395	wt.%	3.724	1.079
Ni	Calc	0.779	0.246	wt.%	2.023	0.639
Mo	Calc	0.828	0.145	wt.%	1.315	0.231
Si	Fixed	1	0	wt.%	5.428	0
Cu	Calc	6.147	0.534	wt.%	14.745	1.28
Ag	Calc	3.362	0.39	wt.%	4.751	0.551
Au	Calc	86.002	2.285	wt.%	66.558	1.769

Figure 5. Spectrum of fluorescence excited by probe beam produced with Mo X-ray tube in metal shell area of the investigated specimen.

was caused by high energy X-ray penetrated trough infill matter and interacted with golden shell after that. For more sensitive acquiring of low energy characteristic X-ray lines, the measurements were performed with another X-ray source based on X-ray tube with Cu anode with 9 kV voltage and 30 mA current operating parameters.

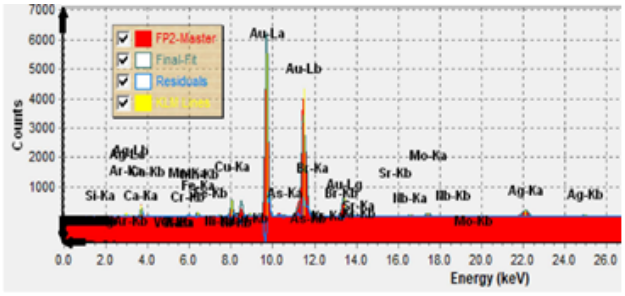

Figure 6. Spectrum of fluorescence excited by probe beam produced with Mo X-ray tube in area of damaged specimen shell.

The voltage was set to be definitely lower than ionization potential for Au L-line and to prevent excitation of Au L-lines and Ag K-lines as well. Measured spectrum is shown in Figure 7. It can be seen that most intensive lines in the measured spectrum are Ca $K\alpha$ and $K\beta$; Cu K-lines are caused by generation both in X-ray tube anode and specimen shell. Application of such parameters allows distinguish in registered spectrum characteristic X-ray lines corresponding to S, that is typically very hard task for measurements in air. Thus, we confirmed that filling material contains Ca and S elements and apparently, this material is gypsum.

As the last part of the XRF study, we measured the fluorescence spectrum of the sample shell in the area of the presence of red paint using Cu X-ray source with voltage increased up to 14 kV. Measured spectrum shown in Figure 8. In this spectrum Hg $L\gamma$ line were distinguished. The resolution of the spectrometer is not sufficient to distinguish clearly Au/Hg $L\alpha$ and $L\beta$ lines

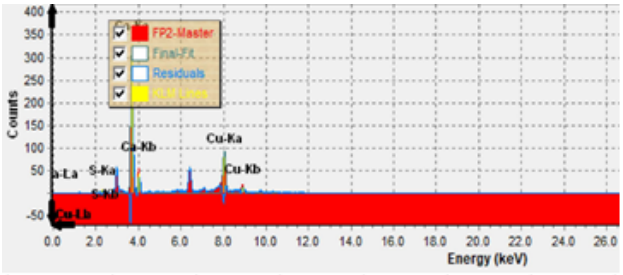

Component Table						
Component	Type	Conc.	Error	Units	Mole%	Error
S	Calc	14.766	5.272	wt.%	17.974	6.417
Ca	Calc	82.496	3.587	wt.%	80.344	3.493
Cu	Calc	2.738	0.181	wt.%	1.682	0.111

Figure 7. Spectrum of fluorescence excited by probe beam produced with Cu X-ray tube operated with 9 kV voltage in area of damaged specimen shell.

since gold and mercury are neighbour chemical elements and, consequently, these lines are mashed. However, $L\gamma$ lines of these elements are clearly distinguishable in acquired spectrum. Thus, Hg was detected in red-painted part of the specimen shell. The presence of mercury may indicate that cinnabar (HgS) was used as a paint that is quite typical for archaeological finds from early ages (Domingo et al., 2012, Mioč et al., 2004, Kendix et al., 2010, Argote et al., 2020, Cotte et al., 2006, Čiuladienė et al., 2020, Tsantini et al., 2018).

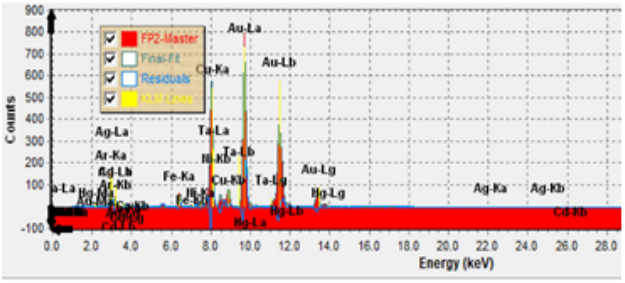

Figure 8. Spectrum of fluorescence excited by probe beam produced with Cu X-ray tube operated with 14 kV voltage in red-painted area of specimen shell.

To define peculiarities and defects of specimen internal structure we perform µ-tomography (µCT) studies using setup in Institute of Applied Problems of Physics (Yerevan, Armenia), which allows obtaining of X-ray images with resolution of about 60 µm. As a source we used tungsten X-ray tube operated at 130 or 150 kV; to suppress the soft part of the spectrum, aluminum and copper filters (d = 1 mm) were used in the first and second cases, respectively; the current equaled 1 mA for both cases. In the first case the X-ray beam was "softer" that provided better contrast between shell and filing material in obtained images and more sensitive analysis of internal structure. In the second case, we suppressed "beam hardening" artefacts that allows better visualization of the structure of metal shell.

Figure 9 shows results of µCT study with source operated in 150 kV mode. Examples of slices obtained in the frontal (Figure 9a), sagittal (Figure 9b) and horizontal planes (Figure 9d), as well as a 3D model obtained from reconstructed tomographic slices (Figure 9c) are shown.

Obtained images allows clear distinguishing of metal shell and

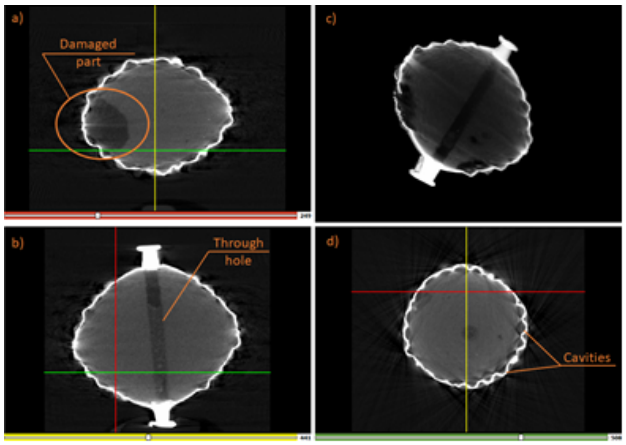

Figure 9. μCT images obtained with 150 kV copper filtered X-ray beam.

filing material. Moreover, several features can be highlighted. For example, an area of lower density at the edge of the specimen in Fig. 9a is clearly visible. This area is located directly behind and adjacent to the damaged part of the metal shell. The density of the filling material apparently changed under the environmental influences, and as a result of microdestructions in this part of the sample. Figure 9b clearly shows through hole in filling material which goes between two "fastenings", it is most likely that this hole was used to thread the fibre to hang the specimen so it could be used as a jewellery or for decoration purposes. In Figure 7d it can be seen that behind the parts of the shell where the protrusions are located there are cavities that are not filled.

Figure 10 demonstrates two slices obtained with "soft" X-ray beam (130 kV and Al filter). These images allow better distinguishing of filling material structure and proves features described above.

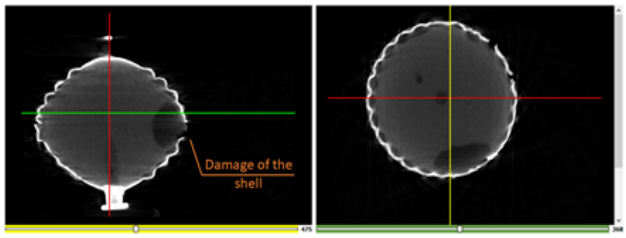

Figure 10. Slices obtained from μCT study with 130 kV aluminium filtered X-ray beam.

3D model of metal shell was separately got from µCT study with "harder" X-ray beam. This model allows detailed visualization of structure and damages of the shell (Figure 11). In the figure a part of model is cut along parasagittal plane.

Both real specimen and model clearly show some kind of scar connecting the top and bottom of the metal shell, that in addition to the cavities found behind the protrusions on the shell, allows conclusion that the sample filler was not poured into the finished metal shell. It is more likely that a core (ball) was formed from the filling material, in which a through hole was made, and then this core was encapsulated with two parts of a metal shell, which were later sealed.

As a final step, the volume of the metal shell and the internal

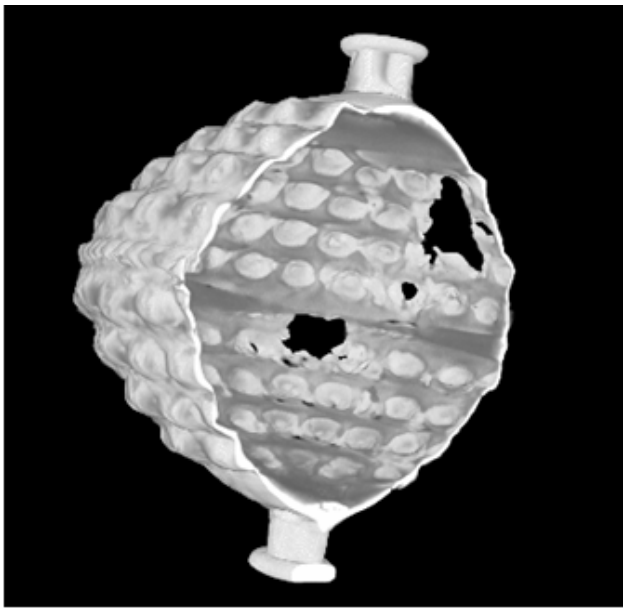

Figure 11. 3D model of specimen shell.

part of the specimen were calculated based on the obtained images. The total volume of the sample equalled V_{sample} = 12.21 cm^3, volume of the metal shell V_{shell} = 0.351 cm^3. These volumes were used to estimate the mass of the sample for the case of our assumptions about its composition and compare with the real mass. For gypsum, a standard density value was taken; the shell density was calculated based on the elemental composition obtained at XRF experiment.

$$\rho_{gypsum} = 2.2\ g/cm^3;$$

$$\rho_{alloy} = 17.44\ g/cm^3\ ;$$

$$M = 32.7g$$

Estimated value are slightly exceeded the actual mass of the sample (31.5 g). However, it should be highlighted that calculation did not account the presence of holes and damages in the specimen. In general, we can say that the mass estimation is quite close to the real value, that indicates the correctness of the assumptions about the specimen composition.

3. Acknowledgement

We gratefully acknowledge all our colleagues for their help in a frame of preparation of this report, especially Elena Atoyants and Liana Zhamagortsyan, who restored artefacts from the excavated burial mound.

This work was supported by the Science Committee of Republic of Armenia, Research project № 23RL-1C037.

References

Argote, D. L., Torres, G., Hernández-Padrón, G., Ortega, V., López-García, P. A., Castaño, V. M., 2020. Cinnabar, hematite and gypsum presence in mural paintings in Teotihuacan, Mexico. *Journal of Archaeological Science: Reports*, 32, 102375.

Avetisyan, P., 2020. On the issues of chronology and periodisation of the Armenian Middle Bronze Age archaeological cultures. *ARAMAZD: Armenian Journal of Near Eastern Studies*, 11.

Brunello, V., Canevali, C., Corti, C., De Kock, T., Rampazzi, L., Recchia, S., Sansonetti, A., Tedeschi, C., Cnudde, V., 2021. Understanding the Microstructure of Mortars for Cultural Heritage Using X-ray CT and MIP. *Materials*, 14(20). https://www.mdpi.com/1996-1944/14/20/5939.

Ceccarelli, S., Redi, M., Alessandra, T., Orazi, N., Guglielmotti, V., Hampai, D., Dabagov, S., 2022. COLOUR CHARACTERISATION FOR THE RESTORATION OF A JAPANESE HANDSCROLL. 12, 109-119.

Čiuladienė, A., Kareiva, A., Raudonis, R., 2020. From model to artefact: Versatile characterization of cinnabar, red lead and realgar red paints for rubrics and miniatures. *Chemija*, 31(4).

Cotte, M., Susini, J., Metrich, N., Moscato, A., Gratziu, C., Bertagnini, A., Pagano, M., 2006. Blackening of Pompeian cinnabar paintings: X-ray microspectroscopy analysis. *Analytical chemistry*, 78(21), 7484–7492.

Dabagov, S., Gladkikh, Y., 2019. Advanced channeling technologies for X-ray applications. *Radiation Physics and Chemistry*, 154, 3-16.

Domingo, I., García-Borja, P., Roldán, C., 2012. Identification, processing and use of red pigments (hematite and cinnabar) in the Valencian Early Neolithic (Spain). *Archaeometry*, 54(5), 868–892.

Gonzalez, V., Cotte, M., Vanmeert, F., de Nolf, W., Janssens, K., 2020. X-ray Diffraction Mapping for Cultural Heritage Science: a Review of Experimental Configurations and Applications. *Chemistry – A European Journal*, 26(8), 1703-1719.

Kendix, E. L., Prati, S., Mazzeo, R., Joseph, E., Sciutto, G., Fagnano, C. et al., 2010. Far infrared spectroscopy in the field of cultural heritage. *Preservation Science*, 7, 8–13.

Mioč, U. B., Colomban, P., Sagon, G., Stojanović, M., Rosić, A., 2004. Ochre decor and cinnabar residues in Neolithic pottery from Vinča, Serbia. *Journal of Raman Spectroscopy*, 35(10), 843–846. http://dx.doi.org/10.1002/jrs.1221.

Morigi, M. P., Casali, F., Bettuzzi, M., Brancaccio, R., D'Errico, V., 2010. Application of X-ray Computed Tomography to Cultural Heritage diagnostics. *Applied Physics A*, 100, 653-661.

Ruvalcaba Sil, J. L., Ramírez Miranda, D., Aguilar Melo, V., Picazo, F., 2010. SANDRA: a portable XRF system for the study of Mexican cultural heritage. *X-Ray Spectrometry*, 39(5), 338-345.

Simonyan, H., 2019. Nerkin Naver – A complex of Archaeological Sites from Middle Bronze Age to the Beginning of Midieval Period. *Russian Academy of Sciences, Institute Archaeology. Caucasian Mountains and Mesopotamian Steppe on the Dawn of the Bronze Age. Festschrift in Honoure of Rauf M. Munchaev's 90th Birthday*, 273-294 (In Russian).

Tsantini, E., Minami, T., Takahashi, K., Ángel Cau Ontiveros, M., 2018. Analysis of sulphur isotopes to identify the origin of cinnabar in the Roman wall paintings from Badalona (Spain). *Journal of Archaeological Science: Reports*, 18, 300-307.

Vaggelli, G., Cossio, R., 2012. μ-XRF analysis of glasses: a non-destructive utility for cultural heritage applications. *Analyst*, 137, 662-667. http://dx.doi.org/10.1039/C1AN15518K.